An AC Microgrid Architecture and Control Strategy to Achieve Stability with Any Type of Load

D. Semënov, G. Mirzaeva, C.D. Townsend, G.C. Goodwin
School of Electrical Engineering and Computer Science, The University of Newcastle, Australia

***Abstract*—This papers presents a theoretical stability study of a newly proposed AC microgrid architecture and its control strategy without droop and communication. The paper proves that the proposed AC microgrid is inherently stable in the presence of any type of load. The paper also proposes a control embellishment, which makes any type of load appear to microgrid as a simple constant current load. Theoretical findings of the paper are validated by extensive simulation results.**

Index Terms – AC microgrid, CPL, CCL, CIL, microgrid control, microgrid stability.

I. Introduction

Today's utility grid is undergoing a transformation from centralized generation model with passive electricity distribution towards smart decentralized networks. AC microgrid is an emerging concept for interconnected distributed generators (DG), battery storage systems (BSS) and local loads.

Advancements in the semiconductors technology, with the consequent drop in prices, turned variable frequency drives, switching power supplies and other power converters into a popular and even typical load type for distribution networks. Such loads will be also present on the load side of an AC microgrids, adding the associated stability issues to the microgrid control problems.

Published research has shown that a realistic microgrid load can be represented as a combination of constant impedance and constant power loads [1]. A constant impedance load (CIL) can be seen as a load, which voltage and current relate to each other via a given and constant impedance. Such loads, for example, heaters and incandescent lamps, typically do not pose a big challenge to power system stability.

Other loads, such as variable frequency drives and various power converters, act as constant power loads (CPL), which change their impedance depending on the input voltage to keep the consumed power constant. That means that an increase in voltage across the converter's terminals will result in a decrease in electric current, and vice versa [2]. This effect, known as a negative incremental impedance, can be a source of instability and may lead to a collapse of the bus voltage [3], [4].

Due to low system inertia, islanded AC and DC microgrids can be easily destabilized and are, therefore, particularly vulnerable to the negative impedance loads [5]. Stability of islanded AC microgrids in the presence of CPL has been investigated by many researchers.

Small-signal behavior of the load depending on the rectifier type is studied in [6], which also determines conditions for small signal stability. Analysis using eigenvalues and Hankel singular values, for different load combinations, is reported in [7]. Admittance-based analysis and Nyquist stability criterion are used in [8], which also proposes three active damping methods. In [9], a nonlinear dynamic model of converter-based CPLs is developed and Popov's stability criterion is applied.

AC microgrids with droop control and virtual impedance has been analyzed in [10] using bifurcation method. In [11] it is proposed to add a virtual resistance into the system, to always keep system poles on the left hand side of the s-plane. A positive effect of a higher line resistance and lower line inductance on a droop controlled AC microgrid is studied in [12]. The use of an external three phase stabilizing inverter is proposed in [13].

The authors of this paper have recently proposed a simple but very effective alternative to a traditional AC microgrid architecture [14]. Instead of using AC frequency and voltage as a microgrid communication method, as in traditional droop control, an implicit communication between the microgrid inverters is achieved by measuring the downstream currents.

The details of this alternative architecture and its control can be found in the companion paper [14]. In this paper it will be shown that the proposed AC microgrid architecture has a significant advantage in terms of system stability. It will be proven theoretically and illustrated by simulations that the proposed AC microgrid is inherently stable in the presence of any type of the load, including constant current load (CCL), constant impedance load (CIL) and constant power load (CPL).

II. Proposed AC microgrid architecture

The alternative topology of AC microgrid proposed in the companion paper [14] is shown in Fig.1a. All distributed generation (DG) inverters operate under closed loop current control, using downstream current measurement (immediately on the right from each DG inverter) as their current references. The left-most, battery storage system (BSS) inverter operates under a tight closed loop voltage control, keeping the capacitor voltage to a set-point value.

As was shown in [14], regardless of the inverter sizes, it is possible to so design the control gains K_j of the individual inverters that the dynamic of each inverter will be described by the following expression:

$$i_{Sj} = D_j i_L \frac{1}{1+s\tau} \tag{1}$$

where i_L is the load current; D_j is the share of the inverter j in the load current; and $\tau = L_1/R_1$ is the time constant of the

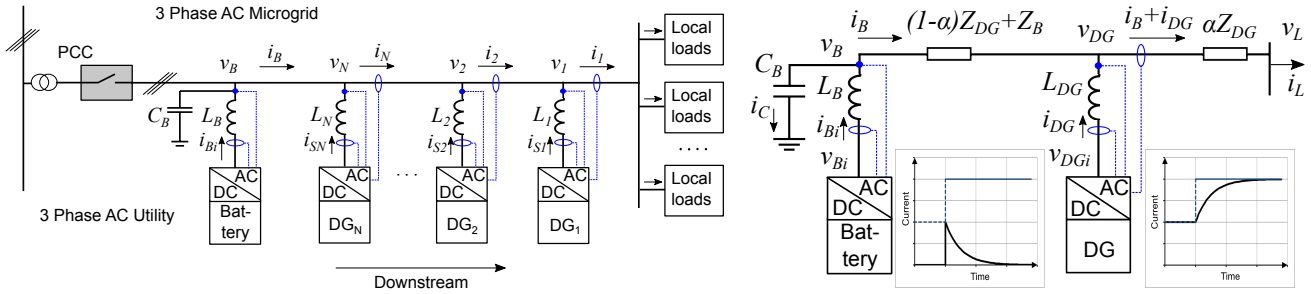

(a) Full circuit with multiple DG and BSS inverters

(b) Equivalent circuit reduced to two inverters

Fig. 1: The proposed AC microgrid architecture and its equivalent circuit.

inverter #1 (the right-most inverter), which is replicated by all other DG inverters by choosing the appropriate gains.

Then the combined current from all DG inverters will be then given by:

$$i_{DG} = \sum_{j=1}^{N} i_{Sj} = \sum_{j=1}^{N} D_j i_L \frac{1}{1+s\tau} = i_L \frac{1}{1+s\tau} \tag{2}$$

Therefore, the combination of N differently rated DG inverters behaves like a single first-order system.

It should be noted that DG inverters, being essentially current-controlled voltage source inverters, cannot respond instantly to a change in the load demand. Therefore, the BSS inverter should act instantly to provide the transient difference between the load current and current supplied by DGs. This is achieved by setting up the BSS inverter as a voltage controlled current source inverter. Then the BSS current i_B is complementing i_{DG} to the total load current i_L:

$$i_B = i_L \frac{s\tau}{1+s\tau} \tag{3}$$

Further, adding line impedances Z_j between the inverters, where:

$$Z_j = R_j + sL_j \tag{4}$$

makes only a small change in the system equivalent circuit. In fact, as shown in [14], the entire microgrid system, including a number of DG inverters and BSS inverters with series impedances of the connecting lines, can be simplified to an equivalent circuit containing only two inverters: one DG and one BSS, as shown in Fig.1b.

The equivalent inverter "DG" in Fig.1b represents all current controlled inverters in the microgrid acting together, while the equivalent inverter "Battery" represents all voltage controlled inverters acting together.

The total line impedance connecting all DG inverters to the load is Z_{DG}, where:

$$Z_{DG} = Z_1 + Z_2 + \ldots + Z_N \tag{5}$$

To account for the fact that different parts of the total DG current flows through different line impedances to reach the load, a coefficient $\alpha < 1$ is introduced so that:

$$Z_1 + Z_2 (D_2 + \ldots + D_N) + \ldots + Z_N D_N = \alpha Z_{DG} \tag{6}$$

Then the BSS voltage can be expressed as:

$$V_B = V_L + \alpha Z_{DG} i_{DG} + (Z_{DG} + Z_B) i_B \tag{7}$$

which is one of the principal equations of proposed in [14] control model for AC microgrid. BSS is chosen as a grid forming power converter, which sets the voltage on the microgrid bus.

III. Stability Study with Different Load Types

It will be assumed in the following stability study that voltage control of the BSS inverters has a much higher bandwidth than current control of DG inverters. In the simulation study presented later in this paper, the bandwidth of the BSS voltage control was selected by two orders of magnitude higher than the bandwidth of the DG current control.

With such a significant difference in bandwidths, the BSS inverter and the DG inverter controls become essentially decoupled. In other words, from the prospective of the DG control, the capacitor voltage V_C can be assumed practically constant, i.e. $V_C = V_{PCC}$. Then the dynamics of the equivalent DG inverter is described by the following differential equation:

$$\tau \frac{di_{DG}}{dt} + i_{DG} = i_L \tag{8}$$

which is the time-domain form of the equation (2).

If the the load current i_L is known, and the DG current i_{DG} is determined from (8), then the BSS current can be found as the difference between these two currents, namely:

$$i_B = i_L - i_{DG} \tag{9}$$

Since the capacitor voltage $V_C = V_{PCC}$, then the load voltage can be found as V_C minus the voltage drops on the series impedances as:

$$V_L = V_{PCC} - (Z_B + Z_{DG}) i_B - \alpha Z_{DG} i_{DG} \tag{10}$$

Using (9), the load voltage can be further expressed as:

$$V_L = V_{PCC} - (Z_B + Z_{DG}) i_L + ((1-\alpha) Z_{DG} + Z_B) i_{DG} \tag{11}$$

It is also clear that in steady state $i_{DG} = i_L$; $i_B = 0$; and $V_L = V_{PCC} - \alpha Z_{DG} i_L$.

In the sequel, we will study the dynamics of i_L, i_{DG}, i_B and V_L for different types of the load. We will start with the CCL model as the simplest case. Then we will explore a more realistic CIL case and, finally, the most challenging CPL

case. For simplicity, we assume that line and load impedances are purely resistive. Extension to a typical RL impedance is straightforward. This would increase the order of the dynamic equations by one, making the analytical solutions bulky, but would not have a significant effect on stability and other important findings of the paper.

Additionally, all the currents and voltages will be illustrated by their one-dimensional components only. This means that all current and voltage space vectors are observed from a synchronously rotating reference frame, and their dq-components are assumed decoupled by a standard decoupling circuit.

A. Constant Current load

If the constant current model is assumed then i_L does not depend on V_L. This means that i_L is driving the other currents. If i_L undergoes a change, then simply i_{DG} can be found from (8); i_B - from (9) or (10); and V_L - from (11).

There is no feedback effect of the change in V_L back on the load current i_L.

For example, if the load current undergoes a step change from i_L^o to i_L^s then, according to equation (8), the DG current is expected to have an exponential response. The solution of the first order linear non-homogeneous equation (8) consists of two parts:

$$i_{DG}(t) = i_{DG}^g(t) + i_{DG}^p(t) \tag{12}$$

where i_{DG}^g is the general solution of the corresponding homogeneous equation; and i_{DG}^p a particular solution of the non-homogeneous equation (8). From examining equation (8), it is clear that:

$$i_{DG}(t) = C_1 e^{-\frac{t}{\tau}} + C_0 \tag{13}$$

where constants C_1, C_0 can be determined from the known initial and final values of the load current as:

$$\begin{aligned} i_{DG}(0) &= C_1 + C_0 = i_L^o \\ i_{DG}(\infty) &= C_0 = i_L^s \end{aligned} \tag{14}$$

Thus, the solution for the DG current will be given by:

$$\begin{aligned} i_{DG}(t) &= (i_L^o - i_L^s)\, e^{-\frac{t}{\tau}} + i_L^s \\ &= i_L^o + (i_L^s - i_L^o)\left(1 - e^{-\frac{t}{\tau}}\right) \end{aligned} \tag{15}$$

The BSS current is determined from (9) as:

$$i_B(t) = (i_L^s - i_L^o)\, e^{-\frac{t}{\tau}} \tag{16}$$

By substituting (15) and (16) into the voltage equation (10), the load voltage can be found as:

$$\begin{aligned} V_L(t) = V_{PCC} - (Z_B + Z_{DG})\,(i_L^s - i_L^o)\, e^{-\frac{t}{\tau}} \\ -\alpha Z_{DG} i_L^o e^{-\frac{t}{\tau}} - \alpha Z_{DG} i_L^s \left(1 - e^{-\frac{t}{\tau}}\right) \end{aligned} \tag{17}$$

The above calculated currents and voltage are shown Figs.2 by black (CCL) plots. It is clear from Fig.2d that, due to the load current change, the load voltage initially drops but then asymptotically reached the new steady value. The load voltage indeed depends on the load current. This is the price to pay for keeping the PCC voltage at a constant value. However, no instability of the load voltage or PCC voltage is observed.

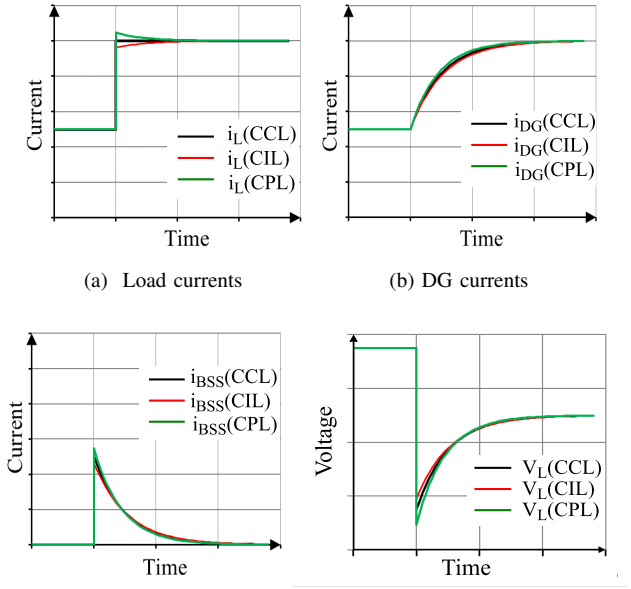

(a) Load currents (b) DG currents

(c) BSS currents (d) Load voltages

Fig. 2: Theoretical transient currents and voltages for different load types.

B. Constant Impedance load

Electric heaters, certain types of lamps and other resistor-like loads will be seen by microgrid as CIL. The same fundamental equations (8)-(11) apply, however, the load current i_L is no longer an independent variable. The objective now is to express i_L in terms of i_{DG} and load impedance Z_L, so that the main dynamic equation (8) can be solved.

From the voltage equation (11) and knowing the load impedance Z_L, the load current can be expressed as:

$$i_L = \frac{V_{PCC} - (Z_B + Z_{DG}) i_L + ((1-\alpha) Z_{DG} + Z_B)\, i_{DG}}{Z_L} \tag{18}$$

which can be solved with respect to i_L as:

$$i_L = \frac{V_{PCC} + ((1-\alpha) Z_{DG} + Z_B)\, i_{DG}}{Z_{DG} + Z_B + Z_L} \tag{19}$$

Substituting expression (19) into the main dynamic equation (8), and separating terms containing i_{DG}, leads to:

$$\tau \frac{di_{DG}}{dt} + i_{DG}\left(1 - \frac{(1-\alpha)\, Z_{DG} + Z_B}{Z_{DG} + Z_B + Z_L}\right) = \frac{V_{PCC}}{Z_{DG} + Z_B + Z_L} \tag{20}$$

which can be simplified into the following form:

$$\tau \frac{Z_L + Z_{DG} + Z_B}{Z_L + \alpha Z_{DG}} \frac{di_{DG}}{dt} + i_{DG} = \frac{V_{PCC}}{Z_L + \alpha Z_{DG}} \tag{21}$$

By introducing a new time constant:

$$\tau' = \tau \frac{Z_L + Z_{DG} + Z_B}{Z_L + \alpha Z_{DG}} \tag{22}$$

equation (21) can be written as:

$$\tau' \frac{di_{DG}}{dt} + i_{DG} = \frac{V_{PCC}}{Z_L + \alpha Z_{DG}} \tag{23}$$

Clearly, the obtained dynamic equation for the DG current in CIL case, is still a linear first order non-homogeneous differential equation. However, its time constant and right-hand side contain a load-dependent impedance Z_L. It can be easily shown that, under steady state condition,

$$i_L = i_{DG} = \frac{V_{PCC}}{Z_L + \alpha Z_{DG}}; \quad V_L = V_{PCC} - \alpha Z_{DG} i_L \quad (24)$$

Consequently, the change in load current (and the proportional change in the load voltage) can only happen due to a change in load impedance.

Say that load impedance undergoes a step change from Z_L^o to Z_L^s. Then, using the same principles as in the CCL case, the solution of the dynamic equation (23) will have the form:

$$i_{DG}(t) = C_1 e^{-\frac{t}{\tau'}} + C_0 \quad (25)$$

where coefficients C_0 and C_1 can be found from the initial and final DG current values:

$$\begin{array}{c} i_{DG}(0) = C_1 + C_0 = \frac{V_{PCC}}{Z_L^o + \alpha Z_{DG}} \\ i_{DG}(\infty) = C_0 = \frac{V_{PCC}}{Z_L^s + \alpha Z_{DG}} \end{array} \quad (26)$$

Finally, the solution of the main dynamic equation for DG current will be given by:

$$i_{DG}(t) = \frac{V_{PCC}}{Z_L^s + \alpha Z_{DG}} + \left(\frac{V_{PCC}}{Z_L^o + \alpha Z_{DG}} - \frac{V_{PCC}}{Z_L^s + \alpha Z_{DG}} \right) e^{-\frac{t}{\tau'}} \quad (27)$$

The corresponding load current, BSS current and load voltage can be found by using expressions (19), (9) and (10), respectively. For the sake of space, the analytical expressions for i_L, i_B and V_L are not provided here but are used to develop the corresponding plots shown in Figs.2 by red (CIL) lines.

For the comparison purpose, the drop in the load impedance is so chosen that it results in the same steady state conditions as in the CCL case.

It is clear from Fig.2d that, if the CIL impedance drops, the CIL load current undergoes an instant step change followed by a further exponential increase. The dynamic of the DG current is slightly slower than for the CCL case due to the difference between τ and τ' evident from (22). The transient BSS current does not reach as a high level and the transient load voltage drop does not reach as a low level, as for the CCL case.

The system remains stable, since the pole of the first order system described by (23) $s = -1/\tau'$ always remains in the left hand side of the complex plane. To summarize, the system behaviour in the case of CIL is very similar to that in the case of CCL, albeit slightly smoother.

C. Constant Power load

When analyzing the microgrid behaviour with CPL, we use a similar approach to the CIL case. Namely, we will express i_L in terms of i_{DG} and load power P_L, so that the main dynamic equation (8) can be solved. Using $i_L V_L = P_L$ and the load voltage expression (11) leads to:

$$i_L \left[V_{PCC} - (Z_B + Z_{DG}) i_L + Z_{eq} i_{DG} \right] = P_L \quad (28)$$

where Z_{eq} is defined as:

$$Z_{eq} = (1 - \alpha) Z_{DG} + Z_B \quad (29)$$

The following quadratic equation for i_L results from (28):

$$(Z_B + Z_{DG})\, i_L^2 - (V_{PCC} + Z_{eq} i_{DG})\, i_L + P_L = 0 \quad (30)$$

The realistic solution of equation (30) is given by:

$$\begin{array}{l} i_L = \frac{V_{PCC} + Z_{eq} i_{DG}}{2\,(Z_{DG} + Z_B)} \\ \quad - \frac{\sqrt{(V_{PCC} + Z_{eq} i_{DG})^2 - 4\,(Z_{DG} + Z_B)\, P_L}}{2\,(Z_{DG} + Z_B)} \end{array} \quad (31)$$

We note that $Z_{eq} i_{DG}$ is a very small value compated to the rest of the terms under the square root. This allows us to use a Taylor series expansion and its linear approximation of the type:

$$\sqrt{(a + bx)^2 - c} \approx \sqrt{a^2 - c} + \frac{ab}{\sqrt{a^2 - c}} x \quad (32)$$

Then the load current i_L can be approximately (with an error of the order of 1%) expressed as:

$$i_L \approx \frac{V_{PCC}\,(1 - f(P_L))}{2\,(Z_{DG} + Z_B)} - \frac{Z_{eq}}{2\,(Z_{DG} + Z_B)} \left(\frac{1}{f(P_L)} - 1 \right) i_{DG} \quad (33)$$

where

$$f\,(P_L) = \sqrt{1 - \frac{4 P_L}{V_{PCC}^2} (Z_{DG} + Z_B)} \quad (34)$$

Then, as per usual, substituting the expression (33) into the main dynamic equation (8), results in:

$$\begin{array}{l} \tau \frac{di_{DG}}{dt} + i_{DG} = \frac{V_{PCC}\,(1 - f\,(P_L))}{2\,(Z_{DG} + Z_B)} \\ \quad - \frac{Z_{eq}}{2\,(Z_{DG} + Z_B)} \left(\frac{1}{f\,(P_L)} - 1 \right) i_{DG} \end{array} \quad (35)$$

Grouping the terms which contain i_{DG} and introducing a modified time constant given by:

$$\tau^{"} = \tau \frac{2\,(Z_{DG} + Z_B)\, f\,(P_L)}{2\,(Z_{DG} + Z_B)\, f\,(P_L) + Z_{eq}\,(1 - f\,(P_L))} \quad (36)$$

and a brief notation:

$$F\,(P_L) = \frac{V_{PCC} f\,(P_L)\,(1 - f\,(P_L))}{2\,(Z_{DG} + Z_B)\, f\,(P_L) + Z_{eq}\,(1 - f\,(P_L))} \quad (37)$$

results in the following compact form of the main dynamic equation for the CPL case:

$$\tau^{"} \frac{di_{DG}}{dt} + i_{DG} = F\,(P_L) \quad (38)$$

It is clear from (38) that $F\,(P_L)$ has the meaning of a steady state DG current.

The load voltage and current can only change as a result of the change in load power. Therefore, it is interesting to see the i_{DG} dynamic following a step change in P_L.

If the load power changes from P_L^o to P_L^s then the corresponding steady state DG currents change from $F\,(P_L^o)$ to

$F(P_L^s)$, which are determined from expression (37). Finally, the solution of the dynamic equation (38) for the CPL case will be given by:

$$i_{DG}(t) = F(P_L^s) + [F(P_L^o) - F(P_L^s)]\, e^{-\frac{t}{\tau^"}} \qquad (39)$$

The resulting analytical solutions for i_L, i_B, i_{DG} and V_L are illustrated by the corresponding plots shown in Figs.2 by green (CPL) lines. For comparison purpose, similar steady state currents are used for all three cases (CCL, CIL and CPL).

It is clear from Fig.2d that, if the CPL power drops, the CPL load current exhibits a small overshoot followed by an exponential decrease.

The dynamic of the DG current is slightly faster than for the CCL case due to that, according to (22), $\tau^"$ is always slightly shorter than τ. The transient BSS current reaches a slightly higher level and the transient load voltage drops to a slightly lower level than those for the CCL case.

The system remains stable, since the pole of the first order system described by (38) $s = -1/\tau^"$ always remains in the left hand side of the complex plane. To summarize, the system behaviour in the case of CPL is very similar to that in the case of CCL, albeit slightly harsher.

D. Concept of dynamic reference

It has been shown so far that, with the proposed microgrid architecture, different types of loads (CCL, CIL and CPL) result in a stable and very similar system dynamics. By using a very simple adjustment, it is further possible to achieve identical system dynamics in all three cases. This can be done by measuring the current i_B supplied by the BSS inverter, and adjusting its voltage reference from V_{PCC} to $V_{PCC} + Z_{eq} i_B$.

Then it can be easily shown that, regardless of the type of the load, the load voltage equation reduces down to:

$$V_L = V_{PCC} - \alpha Z_{DG} i_L \qquad (40)$$

This condition removes dependence of i_L on i_{DG}. The load current can be now independently determined from (40) based on the type of the load. If impedance (in case of CIL) or power (in case of CPL) undergoes a step change, then the load current undergoes an immediate step change, without any exponential rise or decay. The step change of the load current then drives the DG current, according to the main dynamic equation (8).

If the initial and final load currents are i_L^o and i_L^s, respectively, then, regardless of the type of the load, the DG current dynamic will be described by:

$$i_{DG}(t) = i_L^s + [i_L^o - i_L^s]\, e^{-\frac{t}{\tau}} \qquad (41)$$

This makes CCL, CIL or CPL appear identical to the microgrid and, for simplicity, can be all treated as CCL.

IV. Simulation results

A simulation of an AC microgrid developed in accordance with the above principles has been implemented in Matlab/Simulink®. Performance of the AC microgrid has been studied in islanded mode. No droop and no communication between system components have been used.

Parameter	V_{PCC}	L_{DG}	L_{BSS}	C_{BSS}	Z_B	Z_{DG}
Value	240 V	0.1 H	0.01 H	0.001 F	1 Ω	2 Ω

Table I: AC microgrid parameters used in simulation

Parameters of the equivalent microgrid reduced to two inverters (DG and BSS) are given in Table I. It should be noted that the voltage controlled BSS inverters was implemented as a VSI with a fast inner current loop and a slower outer voltage loop. To decouple DG and BSS inverter control loops, the DG control loop was much slower than the outer BSS control loop.

Figs. 3 show simulated transient responses of DG, BSS and load currents, represented by their d-components, under different load types. As can be seen from Figs.3, the transient currents are mostly supplied by the BSS inverter, while the steady state currents are supplied solely by the DG inverter.

Fig. 3a illustrates the microgrid behavior with a CCL load. At $t = 0$ the load current steps from 0 to 5A, and at $t = 15$ ms the load current steps from 5A to 10A. The observed dynamics Of DG and BSS currents corresponds to the theoretical results given by (15) and (16).

Under the simulated CIL scenario, illustrated by Fig. 3b, the load impedance changed from ∞ to 46.75Ω and then to 22.75Ω, which corresponds to the steady state currents 0, 5A and 10A, respectively. Under the simulated CPL scenario, illustrated by Fig. 3c, the load power changes from 0 to 1168.75W and then to 2275W, corresponding to the same steady state currents. In agreement with the theoretical results of Figs.2, the load current exhibits a small undershoot under CIL and a small overshoot under CPL.

The dynamics of the load voltages under the three scenarios are compared in Fig. 3d. In all three cases the load voltage remains stable, with slight difference in dynamics, as expected from the theoretical results.

Finally, Fig.4 illustrates application of the dynamic reference approach to the CPL case. When comparing Fig.4 to Fig.3c it is evident that, when applying the reference adjustment to the BSS inverter, the load current no longer exhibits an overshoot, and the system dynamics become identical to the CCL case.

It can be concluded that the simulation results have shown a very good agreement with the presented theoretical findings.

V. Conclusion

This paper has presented a theoretical stability study of the proposed non-droop AC microgrid architecture and its control strategy. It has theoretically proven that the proposed AC microgrid is inherently stable under any type of loads, including CCL, CIL and CPL.

Furthermore, the paper proposed an embellishment of the BSS inverter control, which makes any type of the load appear to the AC microgrid as a simple constant current load.

The presented theoretical results have been validated by detailed simulations of AC microgrid operation under the scenarios studied in the paper. The paper has confirmed the advantages of the proposed AC microgrid architecture and its control concepts, from the stability prospective.

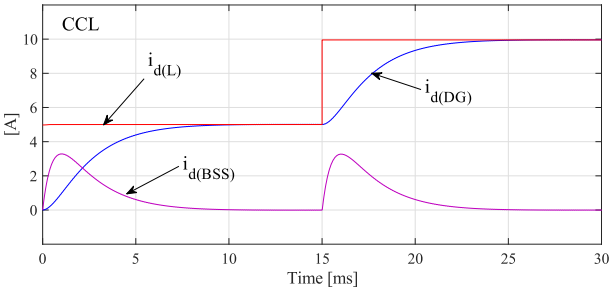

(a) Currents under CCL

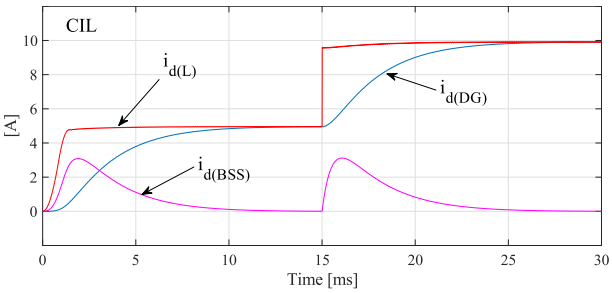

(b) Currents under CIL

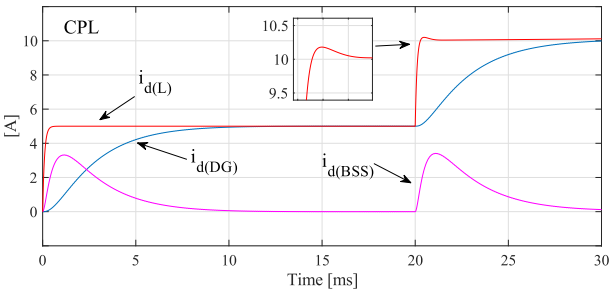

(c) Currents under CPL

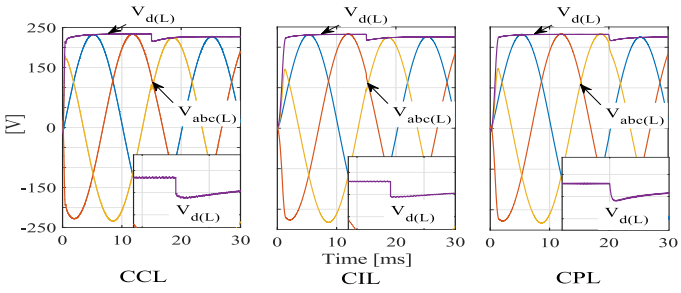

(d) Load voltage waveforms under 3 load types

Fig. 3: Simulated transient currents and voltages for different load types.

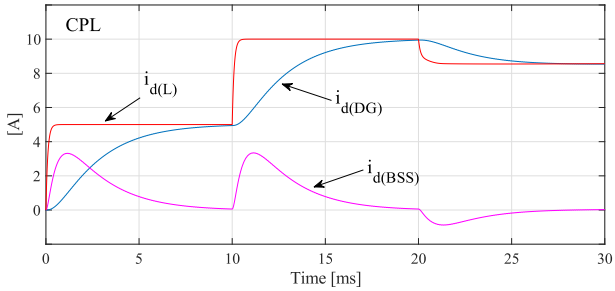

(a) Current transients

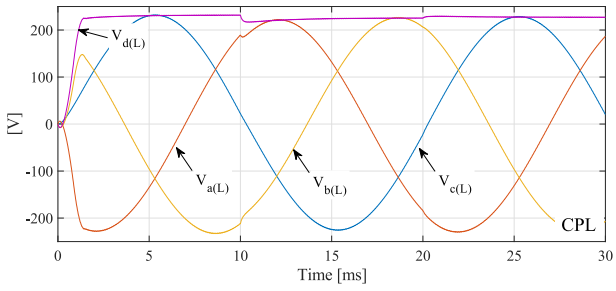

(b) Load voltage waveforms

Fig. 4: Simulated currents and volatges under CPL with dynamic reference.

REFERENCES

[1] S. C. Smithson and S. S. Williamson, "Constant power loads in more electric vehicles - an overview," in *IECON 2012 - 38th Annual Conference on IEEE Industrial Electronics Society*, pp. 2914 – 2922, 2012.

[2] J. Sun, "Impedance-based stability criterion for grid-connected inverters," *IEEE Transactions on Power Electronics*, vol. 26, no. 11, pp. 3075–3078, 2011.

[3] L. Herrera, W. Zhang, and J. Wang, "Stability analysis and controller design of dc microgrids with constant power loads," *IEEE Transactions on Smart Grid*, vol. 8, no. 2, pp. 881 – 888, 2017.

[4] A. M. Rahimi and A. Emadi, "Active damping in dc/dc power electronic converters: A novel method to overcome the problems of constant power loads," *IEEE Transactions on Industrial Electronics*, vol. 56, no. 5, pp. 1428–1439, 2009.

[5] E. Lenz and D. J. Pagano, "Nonlinear control of a three-phase power converter with constant power load in a microgrid," in *2013 Brazilian Power Electronics Conference*, pp. 368 – 373, 2013.

[6] A. Emadi, "Modeling of power electronic loads in ac distribution systems using the generalized state-space averaging method," *IEEE Transactions on Industrial Electronics*, vol. 51, no. 5, pp. 992 – 1000, 2004.

[7] P. E. Raju and T. Jain, "Small signal modelling and stability analysis of an islanded ac microgrid with inverter interfaced dgs," in *2014 International Conference on Smart Electric Grid (ISEG)*, pp. 1–8, 2014.

[8] A. A. Radwan and Y. Abdel-Rady Mohamed, "Modeling, analysis, and stabilization of converter-fed ac microgrids with high penetration of converter-interfaced loads," *IEEE Transactions on Smart Grid*, vol. 3, no. 3, pp. 1213 – 122, 2012.

[9] Karimipour, D., and F. R. Salmasi, "Stability analysis of ac microgrids with constant power loads based on popov's absolute stability criterion," *IEEE Transactions on Circuits and Systems II: Express Briefs*, vol. 62, no. 7, pp. 696 – 700, 2015.

[10] E. L. Cesar, D. J. Pagano, and J. Pou, "Bifurcation analysis of parallel-connected voltage-source inverters with constant power loads," *IEEE Transactions on Smart Grid*, vol. PP, no. 99, pp. 1–1, 2017.

[11] D. M. Vilathgamuwa, X. N. Zhang, S. D. G. Jayasinghe, B. S. Bhangu, C. J. Gajanayake, and K. J. Tseng, "Virtual resistance based active damping solution for constant power instability in ac microgrids," in *IECON 2011 - 37th Annual Conference of the IEEE Industrial Electronics Society*, pp. 3646 – 3651, 2011.

[12] S. Islam and S. Anand, "Eigenvalue sensitivity analysis of microgrid with constant power loads," in *2014 IEEE International Conference on Power Electronics, Drives and Energy Systems (PEDES)*, pp. 1 – 6, 2014.

[13] D. Leblanc, B. Nahid-Mobarakeh, B. Pham, S. Pierfederici, and B. Davat, "Stability analysis and active stabilization by a centralized stabilizer of voltage-source-rectifier loads in ac microgrids," in *2013 IEEE Industry Applications Society Annual Meeting*, pp. 1 – 8, 2013.

[14] G. Mirzaeva, C. D. Townsend, D. Semënov, and C. Goodwin G., "Decentralised control of parallel inverters in an ac microgrid using downstream current as an implicit communication method," in *The 3rd IEEE Southern Power Electronics Conference, SPEC 2017*, 2017.